Contents

Abstract（Chinese） ……………………………………………………………I

Abstract（English） ……………………………………………………………III

Acknowledge……………………………………………………………………….V

Contents…………………………………………………………………………….VI

Table & Figure Captions…………………………………….………………VIII

Chapter 1 Introduction……………………………………………………………1

1.1 Background……………………………………………………………………...1

1.2 Motivation………….……………………………………………………………..2

1.3 Organization of the Thesis……………………..………………………………..4

1.4 References…………………………………………………………………….…...6

Chapter 2 Characteristics Improvement and Carrier Transportation of Cerium-based Gate Dielectrics with Rapid Thermal Annealing

…….….…11

2.1 Introduction…………………………………………………………………….11

2.2 Experimental………..………………………………………………………….12

2.3 Results and Discussion………………………………………………………13

2.3.1 Improved Characteristics of CeO_2 Gate Dielectrics………….....................13

2.3.1.1 C-V Characteristics……………………………………………...….13

2.3.1.2 J-V Characteristics……………………………………………..……13

2.3.1.3 Characteristics of Gate-leakage current density……...…………..14

2.3.1.4 Characteristics of voltage breakdown………...………………….14

2.3.1.5 Time Dependent Dielectric Breakdown………………………….14

2.3.1.6 HRTEM (High Resolution Transmission Electron Microscope) ..15

2.3.1.7 Auger electron spectrometer (AES) analysis…………………….15

2.3.1.8 Electron Spectroscopy for the Chemical Analysis(ESCA)Spectra15

2.3.2 Current Transportation of CeO_2 Gate Dielectrics……………………………16

2.3.2.1 Temperature dependence of leakage current..……………………16

2.3.2.2 Frenkel-Poole (F-P) conduction fitting..…………………………17

2.3.2.3 Fowler-Nordheim (F-N) fitting in the high field region…………17

2.3.2.4 Carrier transportation……………………………………………17

2.3.2.5 The Band Diagram of Al/CeO_2/Si………………………………..17

2.4 Summary………………………………………………………………..17

2.5 References………………………………………………………………29

Chapter 3 Improved Hafnium-based Gate Dielectrics with NH_3 Plasma Treatment and Irradiated TiO_2 Photocatalyst……………………31

3.1 Introduction……………………………………………………………..31

3.1.1 Overview of the high-k dielectrics……………………………….31

3.1.2 Overview of the TiO_2 Photocatalyst……………………………..32

3.2 Experiment procedure…………………………………………………..33

3.3 Results and Discussion…………………………………………………34

3.3.1 SIMS analysis…………………………………………………34

3.3.2 C-V Characteristics…………….....…….………………………..….34

3.3.3 J-V Characteristics…………………………………….....…………35

3.3.4 Characteristics of Gate-leakage Current Density………………….36

3.3.5 Characteristics of voltage Breakdown………….………………….36

3.3.6 Time Dependent Dielectric Breakdown………………….....….….36

3.4 Summary……………………………………………………………...37

3.5 References……………………………………………………………….44

Chapter 4 The preparation of interpoly-oxynitride dielectrics prepared with N_2O RTA and N_2O plasma treatment …………………..…...46

4.1 Introducion…………………………..……………………………..46

4.2 Experiment procedure…………………………………….…………47

4.3 Results and Discussion……………………………………………………….48

4.3.1 J-E Characteristics………………………………………………..…48

4.3.2 Characteristics of Gate-leakage Current Density………………..…49

4.3.3 Characteristics of voltage Breakdown……………………………..49

4.3.4 Time Dependent Dielectric Breakdown………….……………….50

4.3.5 Gate Voltage Shift…………………………………………………….50

4.3.6 Measurement of Effective Barrier Height………………………….51

4.4 Summary……………………………………………………………………...52

4.5 References……………………………………………….…………………64

Chapter 5 Conclusions…………………………….…………………….... 66

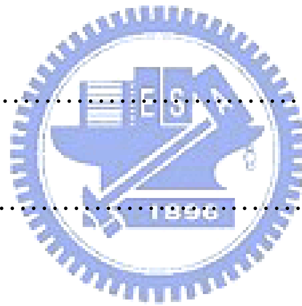

FIGURE CAPTIONS

Chapter 2

Fig.2-1.Key process flows of the fabrication for cerium dielectrics with post-deposition anneal (PDA).

Fig.2-2.The high frequency (100kHz) C-V characteristics of cerium dielectrics with RTA at different temperature.

Fig.2-3.The J-V characteristics of cerium dielectrics with RTA at different temperature.

Fig. 2-4 .Weibull plots of the leakage current density at V_g=1V for the samples treated by RTA.

Fig. 2-5 .Weibull plots of time to breakdown for the samples treated by RTA.

Fig. 2-6: The TEM image of the cerium dioxide without RTA treatment

Fig. 2-7: The TEM image of the cerium dioxide with RTA 600°C

Fig. 2-8: The TEM image of the cerium dioxide with RTA 800°C

Fig. 2-9: The TEM image of the cerium dioxide with RTA 950°C

Fig. 2-10: AES analysis of the as-deposited sample.

Fig. 2-11: AES analysis of the sample treated by RTA 950℃.

Fig. 2-12: Ce3*f* ESCA spectra of the as-deposited sample

Fig. 2-13: Ce3*f* ESCA spectra of the sample treated by RTA 950℃

Fig.2-14: Temperature dependence of leakage current under substrate injection for the sample with RTA at 600℃..

Fig.2-15: Temperature dependence of leakage current under substrate injection for the sample with RTA at 950℃.

Fig. 2-16: Frenkel-Poole (F-P) conduction fitting at V_g=1V for the cerium dielectrics with RTA.

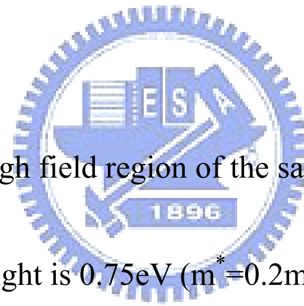

Fig. 2-17: F-N fitting in the high field region of the sample with RTA at 950℃ and the CeO_2/Si barrier height is 0.75eV (m^*=0.2m_0 for Si).

Fig. 2-18: Carrier transportation of the sample with RTA at 600℃ and the trap energy level is about 0.605eV from the conduction band of CeO_2.

Fig.2-19: Band diagram of cerium dielectrics with Al gate.

Chapter 3

Fig. 3-1: (a)(b) The simplified reaction scheme of photocatalysis.

Fig. 3-2: The cross-sectional view and total experimental procedures of the structure.

Fig. 3-3: The SIMS analysis of the as-deposited sample.

Fig.3-4: The high frequency (0.1MHz) capacitance versus gate voltage (C-V) characteristics of these samples.

Fig. 3-5: The J-V characteristics of these samples

Fig.3-6: The Weibull plot of the leakage current density at V_g=-1.5V for these samples.

Fig. 3-7: The Weibull plot of the dielectric breakdown voltage for these samples.

Fig.3-8: The representative plots of current *vs* time during the constant voltage stressing at -3V.

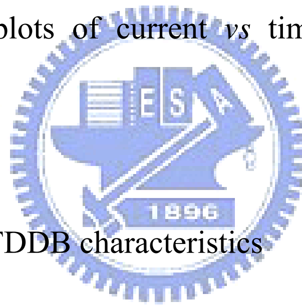

Fig. 3-9: The Weibull plot of TDDB characteristics

Fig.3-10:The negative breakdown field of the projected 10-year lifetime for these samples.

Chapter 4

Fig.4-1:Key process flows of the fabrication for MIM capacitor with interpoly-oxynitride dielectrics..

Fig. 4-2: J-E characteristics of interpoly-oxynitride films of the control sample and the

samples with N_2O RTA and N_2O plasma treatment, under poly Ⅱ positive bias.

Fig. 4-3: J-E characteristics of interpoly-oxynitride films of the control sample and the samples with N_2O RTA and N_2O plasma treatment, under poly Ⅱ negative bias..

Fig. 4-4: Band diagrams of the interpoly-oxynitride dielectrics for the samples with N_2O RTA and N_2O plasma treatment, under (a) poly Ⅱ negative bias and (b) poly Ⅱ positive bias.

Fig. 4-5:Weibull plots of the leakage current density at V_g=+3V for the interpoly-oxynitride dielectrics prepared with N_2O RTA and N_2O plasma treatment.

Fig. 4-6:Weibull plots of the leakage current density at V_g=-3V for the interpoly-oxynitride dielectrics prepared with N_2O RTA and N_2O plasma treatment.

Fig. 4-7: Weibull plots of the dielectric breakdown voltage for the samples treated by N_2O RTA and N_2O plasma treatment under poly Ⅱ positive bias

Fig. 4-8: Weibull plots of the dielectric breakdown voltage for the samples treated by

N_2O RTA and N_2O plasma treatment under poly Ⅱ negative bias

Fig. 4-9: The representative plots of current *vs* time during the constant voltage stressing at V_g=4.2V.

Fig. 4-10: The representative plots of current *vs* time during the constant voltage stressing at V_g=-4.7V

Fig. 4-11: Weibull plots of TDDB characteristics of the samples with N_2O RTA and N_2O plasma treatment, under poly Ⅱ positive bias.

Fig. 4-12: Weibull plots of TDDB characteristics of the samples with N_2O RTA and N_2O plasma treatment, under poly Ⅱ negative bias.

Fig.4-13 The positive breakdown field of the projected 10-year lifetime for these samples.

Fig.4-14 The negative breakdown field of the projected 10-year lifetime for these samples.

Fig.4-15 The graphs of gate voltage shift versus stress time for the samples with RTAN_2O and N_2O plasma treatment.

Fig.4-16 The plots both polarities of extrapolated electric field over the 10-year lifetime (E10y) and the effective barrier height (Φ_B) under poly Ⅱ positive

bias.

Fig.4-17 The plots both polarities of extrapolated electric field over the 10-year lifetime (E_{10y}) and the effective barrier height (Φ_B) under polyⅡnegative bias.

Fig.4-18 The F-N fitting in the high field region of the sample with RTA at 950°C and the measured polyⅡ/SiO_xN_y barrier height is about 1.96eV.